REPORT DOCUMENTATION PAGE

Form Approved OMB No. 0704-0188

1. REPORT DATE *(DD-MM-YYYY)*	2. REPORT TYPE	3. DATES COVERED *(From - To)*
30-01-1998	Paper	

4. TITLE AND SUBTITLE

Design, Optimization and Fabrication of a Free Molecule Micro-Resistojet for Microspacecraft Thrust Generation

5a. CONTRACT NUMBER

5b. GRANT NUMBER

5c. PROGRAM ELEMENT NUMBER

6. AUTHOR(S)

Andrew D. Ketsdever; Dean C. Wadsworth; Stephen E. Vargo; E. Phillip Muntz

5d. PROJECT NUMBER
3058

5e. TASK NUMBER
RF9A

5f. WORK UNIT NUMBER

7. PERFORMING ORGANIZATION NAME(S) AND ADDRESS(ES) AND ADDRESS(ES)

Air Force Research Laboratory (AFMC)
AFRL/PRS
5 Pollux Drive
Edwards AFB CA 93524-7048

8. PERFORMING ORGANIZATION REPORT

9. SPONSORING / MONITORING AGENCY NAME(S) AND ADDRESS(ES)

Air Force Research Laboratory (AFMC)
AFRL/PRS
5 Pollux Drive
Edwards AFB CA 93524-7048

10. SPONSOR/MONITOR'S ACRONYM(S)

11. SPONSOR/MONITOR'S NUMBER(S)
AFRL-PR-ED-TP-1998-037

12. DISTRIBUTION / AVAILABILITY STATEMENT
Approved for public release; distribution unlimited.

13. SUPPLEMENTARY NOTES

14. ABSTRACT

15. SUBJECT TERMS

16. SECURITY CLASSIFICATION OF:			17. LIMITATION OF ABSTRACT	18. NUMBER OF PAGES	19a. NAME OF RESPONSIBLE PERSON
a. REPORT	b. ABSTRACT	c. THIS PAGE			Jay Levine
Unclassified	Unclassified	Unclassified	A		19b. TELEPHONE NUMBER *(include area code)* (661) 275-6179

Design, Optimization and Fabrication of a Free Molecule Micro-Resistojet for Microspacecraft Thrust Generation

Andrew D. Ketsdever

Air Force Research Laboratory
Propulsion Directorate
Propulsion Sciences and Advanced Concepts Division
Edwards AFB, CA 93524-7680

Dean C. Wadsworth

Raytheon STX Corporation
Edwards AFB, CA 93524

Stephen E. Vargo

University of Southern California
Department of Aerospace Engineering
Los Angeles, CA 90089-1191

E. Phillip Muntz

University of Southern California
Department of Aerospace Engineering
Los Angeles, CA 90089-1191

Abstract -- Constellations or platoons of batch-fabricated micro- and nanospacecraft may offer a variety of benefits over large multi-functioning space platforms. Among the major impediments to their introduction are the thrust requirements and power limitations of microspacecraft; low mass, power efficient microthrusters that can deliver accurately controlled μN-sec impulse bits must be developed. The Free Molecule Micro-Resistojet (FMMR) concept that was proposed earlier by Muntz and Ketsdever has been analyzed using direct simulation Monte Carlo numerical simulations and well-established MEMS fabrication techniques. The FMMR combines polysili-

con heating elements to heat a gas expanding through long (~1 cm), narrow (1 to 100 μm wide) slots. Initial simulations suggest that the resistojet can attain a specific impulse of nearly 45 seconds with a thrust level of 0.25 mN for an argon propellant, 10 expansion slots and a heated wall temperature of 600 K. Higher thrust levels can be achieved by increasing the polysilicon heater temperature, changing the slot dimensions, allowing more propellant mass flow through the expanding slots or by changing the propellant. Lightweight construction, device ruggedness and relative ease of fabrication were also important design considerations. Initial fabrication of the FMMR suggests the relative ease of construction using well established MEMS techniques.

I. INTRODUCTION

The growing trend towards the use of large numbers of small spacecraft operating in local clusters or constellations has created a critical requirement for efficient, low power, low mass propulsion systems. Significantly smaller satellites than are being implemented in present low-Earth orbit (LEO) communications constellations are now being proposed [1,2]. Batch-fabricated micro- (mass between 100 kg and 1 kg) or nanospacecraft (mass between 1 kg and 1 g) offer reduced launch costs to orbit due to decreased mass, the availability of a wider variety of launch vehicles, and reduced fabrication costs per satellite [3]. Constellations for communication and surveillance generally require nominal satellite spacing and orientation, making active propulsion systems necessary. Small satellites are not only mass limited but also seriously power limited due to decreased surface area available for solar panels. For the mass range below 50 kg, a figure of merit is 1 Watt/kg available for propulsion, although this could be increased during orbital transfer or plane change maneuvers [4]. It is clear that micropropulsion systems will require similar

microelectromechanical system (MEMS) design considerations as other satellite subsystems and components.

There is a growing realization that in many cases microthrusters will not be simply scaled down versions of existing thrusters. For example, to maintain efficiency at small scales for chemical thrusters requires a significant increase in operating pressure to maintain equivalent levels of frozen flow and viscous losses [5]. Typical nozzle expansions require throat diameters on the order of 10 μm which are easily plugged by particulates. For ion electric propulsion systems, the increased surface-to-volume ratio as size decreases makes the scaling of electric thrusters to small sizes, while maintaining efficiency, extremely difficult. Magnetic field scaling and acceleration grid production problems also exist for small ion thrusters [6,7].

A free molecule micro-resistojet (FMMR) thruster concept first discussed by Muntz and Ketsdever [8] which offers several distinct advantages over conventional microthruster concepts for attitude control and station keeping maneuvers is further developed in this paper. The FMMR combines MEMS fabrication techniques with simple, lightweight construction as shown schematically in Fig. 1. The FMMR consists of a polysilicon thin film heating element at a temperature T_w and a long exhaust slot. A slot is chosen as an advantage over a small nozzle expansion because of the possibility of contaminants catastrophically plugging the small orifice (typically on the order of 10 μm in diameter). Characteristic dimensions for the FMMR design considered in this work are shown in Fig. 1.

Free molecule flow is a limiting case where the molecular mean free path is very large compared to a characteristic dimension in the flow (large Knudsen number). In the case of the FMMR, the characteristic dimension is taken as the slot width. The free molecule condition requires that the slot width, w, be less than 1/4 of the molecular mean free path in the stagnation chamber. At these conditions, collisions between molecules are infrequent with little viscous loss due to the "nozzle" geometry making an easily micromachined slot an appropriate expansion configuration. The free molecule condition is chosen for the additional important benefit of reduced propellant storage pressure therefore easing valving requirements. The design requirement is to arrange that the last surface contacted by a molecule before it exits through the slot is the heated surface. This requirement suggests that the spacing between the heating element and the expansion slot be on the order of the mean free path of the stagnation gas (~ w). The FMMR concept is scalable to high thrust applications by arraying the heater elements and slots as shown in Fig. 1(b).

In the present study, we use parametric numerical simulations to investigate the generation of thrust made possible by local/ differential surface heating of the rarefied propellant gas in a relatively easily-fabricated and robust MEMS structure.

II. THEORY

The thrust, $\Im$, from an electrothermal thruster such as the FMMR is given by [9]

$$\Im = \dot{m} I_{sp} g_o \quad (1)$$

where $\dot{m}$ is the propellant mass flow [kg/sec], I_{sp} is the specific impulse [sec] and g_o is the standard gravitational acceleration at sea level [m/sec^2] . The specific impulse is defined as the total impulse (integrated thrust) per unit mass of the propellant and is a measure of the propellant utilization efficiency.

In free molecule flow, the specific impulse, based on the free molecule results for mass flow and momentum flux, is given by

$$(I_{sp})_{FM} = \frac{\sqrt{\frac{\pi}{2}\frac{k}{m}T_o}}{g_o} \quad (2)$$

where T_o is the propellant gas stagnation temperature near the expansion slot (in general $T_o \neq T_w$) and m is the propellant molecular mass. The ratio of the specific impulse for limit expansion through an ideal nozzle to that for free molecule flow through a slot depends on the propellent but is approximately 2. The efficiency losses associated with free molecule slot expansion versus limit continuum ideal nozzle expansion can be countered from a systems point of view through trade offs such as design simplicity, reduced propellant storage pressure, and the minimization of catastrophic nozzle clogging due to particulate contaminants.

III. CALCULATIONS

The simple one-dimensional, stationary gas, free-molecular results are expected to be useful in basic design, however, the actual micro-resistojet involves multidimensional transitional rarefied

gas flow, and more sophisticated analysis methods are required for accurate performance predictions. The direct simulation Monte Carlo (dsMC) method [10] provides a means to simulate the flow of a general rarefied gas at the molecular level. Many of the input models required in dsMC, such as gas-surface interaction, are topics of current research. Even with these uncertainties, the detailed information available from direct parametric simulations are indispensable to the design process. Parametric variation of input model features can also be used to assess sensitivity of performance predictions to these uncertainties. The present dsMC implementation has been applied to several problems related to micro-resistojet design, where the key feature to be resolved is the development of a bulk motion and the generation of thrust in a confined rarefied gas due to differential heating of a bounding surface [11-14].

The two-dimensional computational domain for the nominal geometry (oriented such that thrust is generated in the horizontal direction) is shown in Fig. 2. The geometry is symmetrical about the nozzle centerline. Boundary AB is an open inlet. Molecules entering are selected from a drifting equilibrium distribution, with the drift velocity iteratively updated to obtain the input plenum pressure at the boundary. Boundary IJ is a plane of symmetry for this periodic, multislot configuration. The farfield vacuum boundary DJ is placed approximately 10 nozzle widths downstream of the nozzle exit. Each wall surface is nominally a fully-accommodating diffuse reflector defined by an input temperature T_w. For the present, the key feature that enhances bulk flow in the propellant gas is the differential heating of the pedestal surface FI relative to that of the nominal plenum surface temperature. More accurate simulations, which iteratively couple the gas and structural heat transfer properties and thus eliminate the need for an input surface temperature distribution, will be reported at a later time [15].

The computational domain is divided into a grid consisting of 10 zones, each with locally varying cell sizes. For the present highly rarefied operating conditions, the dsMC requirement that the nominal cell size be on the order of the local molecular mean free path is easily met. The requirement that the simulation timestep be small relative to the typical collision time is met for the same reasons. Gas-gas collisions are simulated using the VHS model.

The code is instrumented to directly sample and spatially resolve the flux of molecular mass, momentum, and energy through an arbitrary flowfield plane, here chosen to typically be the slot throat (GG'), or the slot exit (HH'). These quantities are also sampled at all surface elements. These flux data allow division/assignment of thrust contributions and losses to various components of the structure, such as the slot walls (GH).

The nominal simulation used 2000 cells, 200000 particles, and was run for 2000 unsteady timesteps and for 10000 additional steady-state timesteps during which sampling of the flowfield occurred. The unsteady portion of the solution corresponded to approximately 200 acoustic times, based on the plenum speed of sound and the slot width. Nominal local cell sample sizes were on the order of 200000, and flux plane sample sizes were 10^6.

IV. RESULTS

Design parametrics were carried out by varying the heating element wall temperature, T_w, heating element surface area, propellant used, stagnation pressure and slot divergence angle.

Each case is for a gas expansion slot width, w, of 100 μm and a slot depth of 250 μm. The heater element width is 3w or 300 μm wide (as optimized during the parametric study) and the gas stagnation temperature far removed from the heating element is 300 K. Fig. 3 shows typical flowfield results for the nominal case (T_w = 600 K, T_o = 300 K). The contours consist of raw data, with each "pixel" corresponding to a flowfield cell, and give an indication of grid resolution. The left half of the figure shows translational temperature contours. At this rarefaction, "slip" phenomena are expected to be large. This feature is confirmed by the peak temperature in the gas near the pedestal remaining much lower than the pedestal wall surface temperature. The right half of the figure shows axial velocity contours. The acceleration of the gas due to the slot expansion is evident, while near the slot wall large velocity slip occurs.

Fig. 4 shows the effect of pedestal surface temperature on performance for an argon propellant gas. The trend toward improved I_{sp} as temperature is increased is less than, but still comparable to, that predicted by the free-molecular results (Equation (2), $\sqrt{T}$). Fig. 5 also shows the effect of propellant gas (molecular mass, m) on performance for T_w = 600 K. The trend is also comparable to that predicted by the free-molecular results (Equation (2), $\sqrt{1/m}$). The polyatomic ammonia has been modeled assuming zero internal energy. The gas-surface interaction process is expected to increasingly influence performance for more complex molecules.

Fig. 6 shows the effect of slot divergence angle, α, on performance for T_w = 600 K. The case of α = 54.74 degrees corresponds to that etchable for the <100> plane of crystalline Si. Comparison of the axial components of slot surface pressure and shear forces indicate that the slot expansion

provides a net positive increment to performance for the smaller angles and lengths considered. The relatively large shear losses indicate that for these highly rarefied flows, small expansion ratios (or short slot heights) are preferable. This same design criteria arises in continuum analyses of less rarefied nozzle flows [16]. The limiting case of 90 degrees results in a constant width slot, where only shear losses arise, leading to poor performance.

V. ESTIMATED THRUSTER PERFORMANCE

For a nominal case thruster with a slot length of 1 cm, the FMMR design produces a thrust of approximately 0.025 mN per slot as derived from the dsMC results. Therefore, a thruster arrangement of 10 slots produces a total thrust of 0.25 mN at a heated wall temperature of 600 K. For applications which require large thrust levels, the stagnation pressure, the stagnation wall temperature, and the total number of slots can all be increased to achieve the desired thrust level.

As mentioned earlier, the FMMR can be scaled to larger thrust levels by increasing the pressure (smaller Knudsen number for a constant slot width of 100 μm) in the stagnation region as shown in Fig. 7 for T_w = 600 K. The thrust is calculated assuming a single expansion slot 1 cm long. Extremely low values of thrust which are important for incremental maneuvers and critical pointing can be achieved by simply reducing the pressure in the stagnation region without sacrificing efficiency. Arbitrarily small impulse bits (I-bit) are possible by this simple strategy with easily achievable valve cycle times. Fig. 7 shows the effect on the specific impulse for T_w = 600 K as the stagnation pressure is decreased or the Knudsen number increases. The calculated I_{sp} of the FMMR increases slightly as the Knudsen number decreases and will most likely asymptote to the

value for a sonic, continuum orifice. As shown in Fig. 7, the enhanced performance comes at the expense of higher thrust for a constant slot width as the Knudsen number decreases. The impulse bit is based on the thrust and the valve actuation time implying that the higher thrust level requires a shorter valve response time for the same impulse bit. Since microspacecraft will require impulse bits on the order of μN-sec, reducing a microthruster's thrust level, without sacraficing much in specific impulse, is essential to maintain easily achievable valve actuation times. Fig. 7 indicates the flexiblity of the FMMR in meeting several different mission requirements on the same spacecraft.

A dsMC parametric study was done to optimize the heating element pedestal width in terms of the thruster performance. As expected, the calculated specific impulse asymptoted to the free molecule theory value as the heated surface area increased. A pedestal width of 3w or 300 μm appeared to be a reasonable compromise between the performance and the input heating power cost and was used throughout the calculations.

VI. FABRICATION TECHNIQUES

This section focuses on the fabrication steps needed to process and assemble a proof-of-concept FMMR design similar to that depicted in Fig. 1. The device is a result of a design analysis based on dsMC numerical simulations and well-established MEMS fabrication techniques. Lightweight construction, device ruggedness and relative ease of fabrication were also important design considerations. The proof-of-concept FMMR, composed of silicon and Pyrex 7740® Corning glass wafers, is assembled in a stacked configuration utilizing several wafer bonding techniques. In

terms of minimizing heat transfer losses, a device constructed of these materials is by no means optimal but allows simplified characterization of a prototypical device. A preliminary heat transfer analysis suggests that a power efficient thruster can be constructed using suspended heating elements (i.e. no heating element support pedestal) or pedestals of relatively thick insulating material. The use of low thermal conductivity materials such as ceramic and quartz appears feasible; however, a thorough study of MEMS-based or conventional fabrication methods of these materials needs to be researched.

The prototype FMMR currently under consideration is composed of five parts in the following top-to-bottom stacking order: 1) silicon wafer with etched slots with a 54.74° gas expansion angle, 2) silicon wafer providing the proper slot to heater spacing, 3) silicon wafer with patterned heaters and etched gas passages, 4) Pyrex wafer utilized as a gas plenum section, and 5) Pyrex wafer with a joined glass tube serving as the gas feedthrough. Part Numbers 1 through 4 are fabricated based on MEMS processing steps whereas Part Number 5 is fabricated by conventional methods.

A. Processing Steps

The following processing steps result in thirteen 8 mm long slots spaced 200 μm apart on a <100> crystallographic orientated 250 μm thick silicon wafer. Each slot has sidewalls that are sloped at an angle of 54.74° resulting in a slot width of 100 μm. To achieve the proper slot sidewall angular conditions, the isotropic wet chemical etchant ethylenediamine-pyrocatechol-water (EDP) is selected [17]. Since only desired areas of the wafer are to be etched, a few masking steps are needed which include the deposition of a 100 nm layer of silicon nitride on the wafer by Low Pressure Chemical Vapour Deposition (LPCVD) to protect both wafer sides and the spinning of a

photoresist pattern on the top silicon nitride surface. The exposed silicon nitride areas are etched anisotropically using a reactive ion etching (RIE) plasma of CF_4 and O_2. Once the silicon surface has been exposed the photoresist is stripped and the wafer is placed in a heated type-F EDP bath. After etching completely through the wafer, the silicon nitride layers are removed using the same RIE step. A scanning electron microscope (SEM) micrograph of the initial processing of a 400μm deep expansion slot is shown in Fig. 8. The spacer between the expansion slots and the heating element pedestals is fabricated by similar processing steps as the expansion slots using a 100 μm thick silicon wafer. The etching of this wafer removes most of the central silicon area leaving a thin perimeter for bonding of the expansion slots to the heater section.

The heater section consists of patterned heaters and gas flow trenches on a 400 μm thick silicon wafer. The heaters are processed by depositing a 1 μm layer of LPCVD polysilicon on the wafer. Patterning of the polysilicon layer results in the placement of the heating elements directly beneath the fabricated expansion slots as shown in Fig. 1. Heater formation results by spinning on a layer of photoresist which is patterned and anisotropically etched using a RIE plasma of SF_6 . The etch provides a heating element that is 300 μm wide and roughly 110 mm (8 mm per pass) long that passes beneath each slot in a serpentine-like pattern. The heating elements are supported by 300 μm wide, 8 mm long and 250 μm tall pedestal structures in the silicon wafer. The pedestals ensure that most of the gas escaping the stagnation region through the expansion slots have collided with the heated top surface which is critical for thruster performance. Pedestal formation is achieved using a deep RIE utilizing an inductively coupled plasma of SF_6 and C_4F_8 [18]. A deep RIE of this type provides a method for the etching of highly anisotropic (~90° sidewalls) structures in silicon using only photoresist as a mask. A SEM micrograph of the initial processing of

the pedestals is shown in Fig. 9. The pedestals shown are roughly 240 μm tall with a pedestal-to-pedestal spacing of 300 μm. Gas passages, which are etched slots, are inserted between the pedestals to allow gas to flow between adjacent wafers. These slots are created using the same deep RIE process used for the pedestal formation except from the opposite side of the wafer. When completed a system of 14 trenches that are each 8 mm long and 270 μm wide are placed on either side of the heaters. These trenches provide an open area that is greater than the area provided by the gas inlet tube to prevent flow restrictions.

The gas plenum section is made from a 3 mm thick Pyrex wafer. The processing of this wafer begins with evaporating a layer of chrome/gold on both sides of the wafer to serve as an etch mask. Photoresist layers are spun on and patterned to define a cavity. The exposed chrome and gold layers are each etched in their appropriate etchants. Once the Pyrex surfaces are exposed, the wafer is placed in a solution of hydrofluoric acid (HF) that etches completely through the wafer. The final step for the plenum wafer involves etching the masking chrome/gold layer resulting in the majority of the wafer being removed leaving a thin perimeter for bonding. The glass inlet section is conventionally fabricated using a 6 mm outside diameter Pyrex tube fused to a 3 mm thick Pyrex wafer.

B. Assembly

The assembly of the five parts is accomplished using anodic, fusion and organic wafer bonding techniques [19]. The expansion slot wafer, the silicon spacer and the heating element wafer are bonded to each other using silicon-silicon fusion bonding. The silicon wafers are anodically bonded to the Pyrex plenum. The anodic bond is formed when the two parts are placed in contact,

heated to a temperature of 450 °C and a differential voltage of order 700 V is applied to the two parts. The last step in the assembly involves organically bonding (with epoxy sealant) the gas inlet wafer to the rest of the assembly.

VII. CONCLUSION

The FMMR concept exemplifies how a novel concept is applicable to small scale thrusters. System accommodations often outweigh more narrowly focussed performance issues when propulsion systems are considered for spacecraft operations. Although the FMMR's performance may not be as good as an ideal continuum expansion nozzle, the FMMR exibits several advantages over traditional small scale thrusters in reduced propellant storage pressure, the abatement of catastrophic nozzle plugging, ease and flexibility of construction and reduced valve actuation requirements for small impulse bits.

An iterated design concept has been developed for the FMMR using parametric studies with the direct simulation Monte Carlo numerical technique. The nominal design calls for a 100 μm wide by 8 mm long slot with an expansion angle of 54.74°. The heating element optimum width is found to be approximately three times the slot width (300 μm) with a surface temperature between 600 and 1200 K. Calculations using an argon propellant at a stagnation temperature of 600 K show that a thrust level near 0.25 mN at a specific impulse of approximately 45 seconds can be achieved for a thruster configuration utilizing 10 expansion slots and associated heating elements. For higher thrust requirements, the slot width can be changed to allow for higher mass flows from the thruster while still maintaining the free molecule condition. For propellant storage

ease, future thruster designs using ammonia or water propellants will be investigated. For these cases, the gas-surface interaction models used in the dsMC code are expected to dominate the results due to coupling with internal energy modes.

REFERENCES

1. S. Janson, H. Helvajian, and E. Robinson, "The Concept of Nanosatellite for Revolutionary Low-Cost Space Systems," paper IAF-93-U.5.573, 44th Congress of the International Astronautics Federation, Graz, Austria, October 1993.

2. J. Mueller, "Thruster Options for Microspacecraft: A Review and Evaluation of Existing Hardware and Emerging Technologies," paper AIAA 97-3058, 33rd Joint Propulsion Conference, Seattle, Washington, July 1997.

3. S. Janson, "Batch-Fabricated Resistojets: Initial Results," paper IEPC 97-070, 25th International Electric Propulsion Conference, Cleveland, Ohio, August 1997.

4. S. Janson, "Chemical and Electric Micropropulsion Concepts for Nanosatellites," paper AIAA 94-2998, 30th Joint Propulsion Conference, Indianapolis, Indiana, June 1994.

5. R. Bayt, A. Ayon, and K. Breuer, "A Performance Evaluation of MEMS-based Micronozzles," paper AIAA 97-3169, 33rd Joint Propulsion Conference, Seattle, Washington, July 1997.

6. G. Yashko, G. Giffin, and D. Hastings, "Design Considerations for Ion Microthrusters," paper IEPC 97-072, 25th International Electric Propulsion Conference, Cleveland, Ohio, August 1997.

7. J. Mueller, W. Tang, W. Li, and A. Wallace, "Micro-Fabricated Accelerator Grid System Feasibility Assessment for Micro-Ion Engines," paper IEPC 97-071, 25th International Electric Propulsion Conference, Cleveland, Ohio, August 1997.

8. E.P. Muntz and A. Ketsdever, "Microspacecraft Exhaust Plumes, Thrust Generation and Envelope Expansion to Lower Altitudes," AFOSR Microthruster Workshop, San Diego, CA, July 1997.

9. G. Sutton, *Rocket Propulsion Elements: An Introduction to the Engineering of Rockets*, Sixth Edition, John Wiley & Sons, New York, 1992.

10. G. Bird, *Molecular Gas Dynamics and the Direct Simulation of Gas Flows*, Clarendon Press, Oxford, 1994.

11. D.C. Wadsworth, D.A. Erwin, and E.P. Muntz, "Transient motion of a confined rarefied gas due to wall heating or cooling", J. Fluid Mech., 248, 219-235, 1993.

12. D.C. Wadsworth and E.P. Muntz, "A Computational Study of Radiometric Phenomena for Powering Microactuators with Unlimited Displacements and Large Available Forces," J. Microelectromechanical Systems, 5, 59-65, 1995.

13. D.C. Wadsworth, E.P. Muntz, G.Pham-Van-Diep, and P.Keeley, "Crookes' radiometer and micromechanical actuators," in Rarefied Gas Dynamics, Proceedings of the 19th International Symposium, Oxford 1994, J. Harvey and G. Lord, Eds. 1995, Oxford University Press, 708-714.

14. D.C. Wadsworth, "Slip effects in a confined rarefied gas, {I}: Temperature slip," Phys. Fluids A, 5, 1831-1839, 1993.

15. D. C. Wadsworth, "Coupled Aerothermodynamic Analysis of High-Temperature Micro-nozzles," in preparation.

16. W. J. Rae, "Study of Low Density Nozzle Flows, with Application to Microthrust Rockets," AIAA J., 9, 811-820, 1971.

17. K. Petersen, "Silicon as a Mechanical Material," Proc. of the IEEE, 70 (5), May 1982.

18. J. Bhardwaj and H. Ashraf, "Advanced silicon etching using high density plasmas," Micromachining and Microfabrication Process Technology - SPIE, 2639, 224-233, 1995.

19. S. Sze, *Semiconductor Sensors*, John Wiley & Sons, New York, 1994.

FIGURE CAPTIONS

Fig.1: (a) Cross sectional view of Free Molecule Micro-Resistojet (FMMR) configuration. (b) Arrayed expansion slot and heating element configuration for microspacecraft propulsion system.

Fig. 2: Computational geometry.

Fig. 3: Flow field contours for nominal FMMR operating conditions. Left side: Translational temperature contours. Right side: Axial velocity conours.

Fig. 4: FMMR specific impulse as a function of heating element wall temperature T_w for argon. Theoretical line is calculated from equation (2).

Fig. 5: FMMR specific impulse for various propellants for T_w = 600 K. Theoretical line is calculated from equation (2).

Fig. 6: FMMR specific impulse for an argon propellant as a function of slot expansion angle for T_w = 600 K and assuming a slot wall temperature of 300 K.

Fig. 7: FMMR performance as a function of argon stagnation pressure or Knudsen number for T_w = 600 K. The specific impulse free molecule limit was calculated using the dsMC technique with no intermolecular collisions.

Fig. 8: SEM micrograph of initial processing of expansion slot configuration.

Fig. 9: SEM micrograph of initial processing of heating element pedestal configuration.

BIOGRAPHY

Andrew D. Ketsdever received the B.S., M.S. and Ph.D. in aerospace engineering at the University of Southern California in 1990, 1992, and 1995, respectively.

He is currently a Senior Scientist with the Air Force Research Laboratory at Edwards AFB, CA. His research interests include experimental techniques in rarefied gas flows, spacecraft environmental interactions, gas-surface interactions and the development of unique micropropulsion concepts.

Dean C. Wadsworth received the B.S. in aerospace engineering from the University of Colorado, the M.S. in applied mechanics and engineering science from the University of California, San Diego, and the Ph.D. in aerospace engineering from the University of Southern California in 1985, 1989, and 1993, respectively.

He is currently a Principal Scientist with Raytheon STX. His research interests are in the development and application of multidisciplinary simulation tools for nonequilibrium and microelectromechanical gas dynamic flows.

Stephen E. Vargo received the B.S. and M.S. in Aerospace Engineering from the University of Southern California in 1994 and 1995, respectively.

He is currently a research assistant at the University of Southern California in the Department of Aerospace Engineering. His research interests include the study of non-equilibrium flows and the design and fabrication of various MEMS devices.

E. Phillip Muntz received the B.A.Sc. and the Ph.D. degrees for the University of Toronto in 1956 and 1961, respectively.

He joined the faculty of the University of Southern California in 1969 and is currently the A.B. Freeman Professor of Engineering and the Chairman of Aerospace Engineering. His research interests are in the study of nonequilibrium gas flows, the application of nonequilibrium phenomena in micromechanical devices and the development of electric micropropulsion techniques.

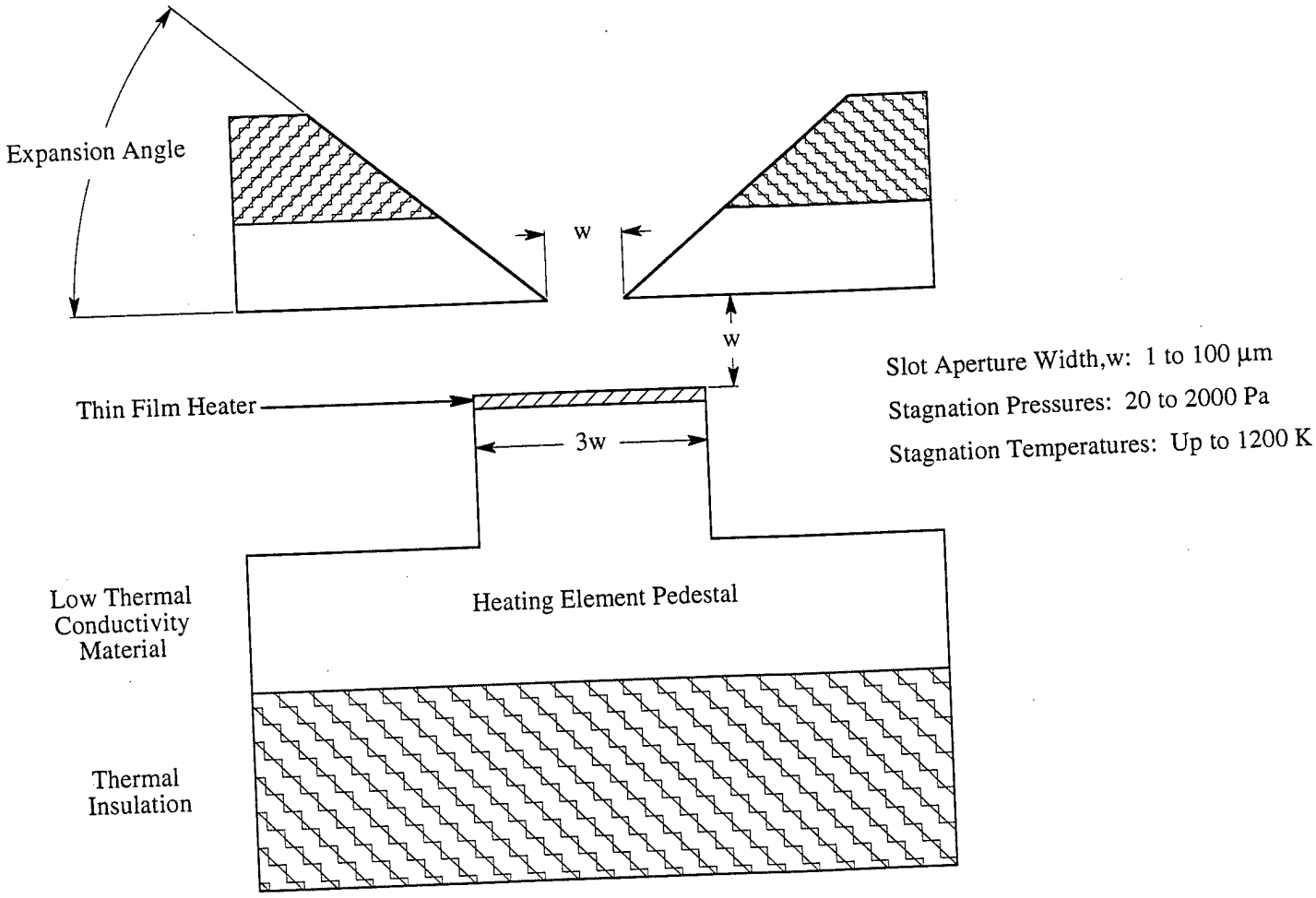
Expansion Angle
w
w
Thin Film Heater
3w
Slot Aperture Width,w: 1 to 100 μm
Stagnation Pressures: 20 to 2000 Pa
Stagnation Temperatures: Up to 1200 K
Low Thermal Conductivity Material
Heating Element Pedestal
Thermal Insulation

Figure 1 (a)

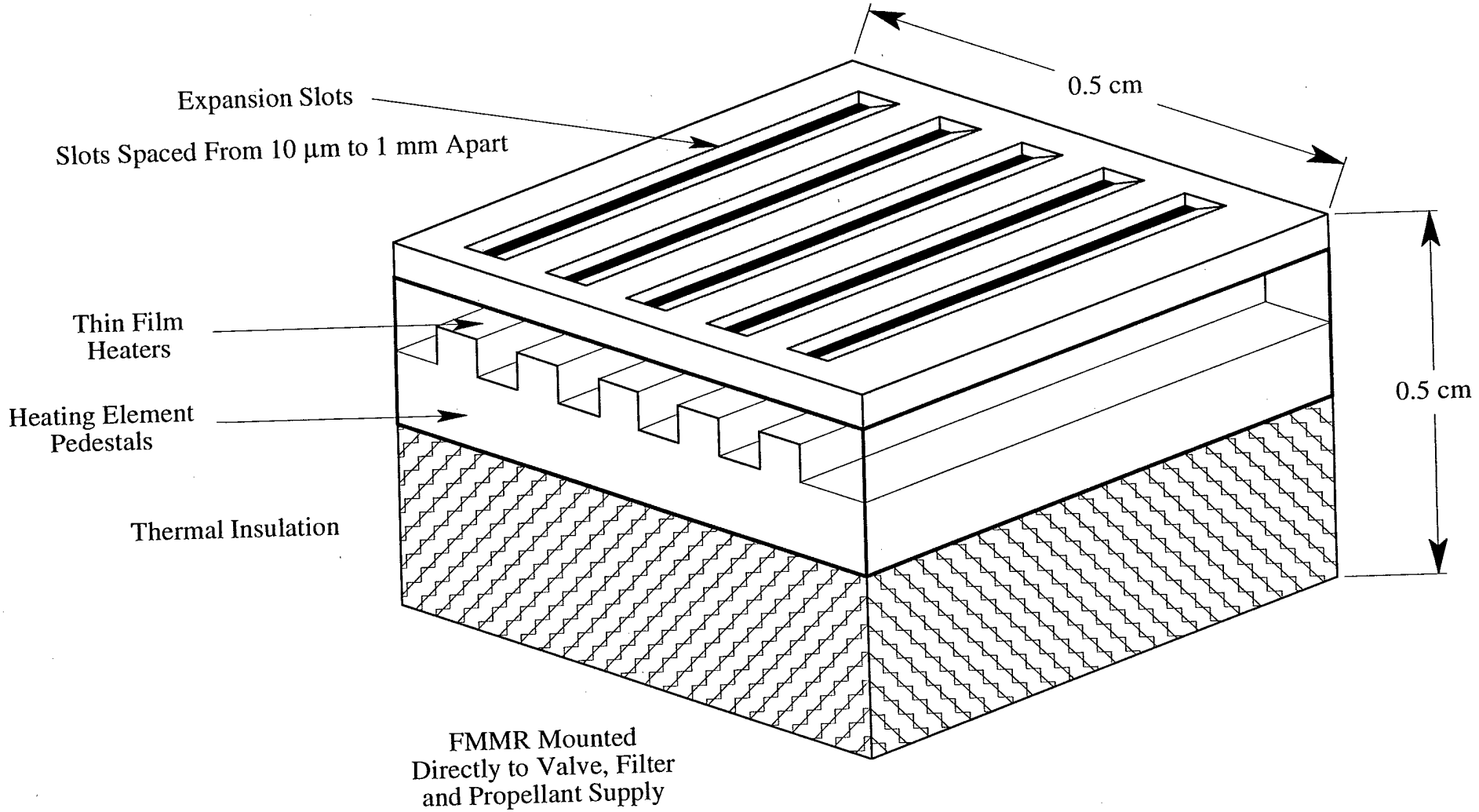
Expansion Slots
Slots Spaced From 10 µm to 1 mm Apart
0.5 cm
Thin Film Heaters
Heating Element Pedestals
Thermal Insulation
0.5 cm
FMMR Mounted Directly to Valve, Filter and Propellant Supply

Figure 1 (b)

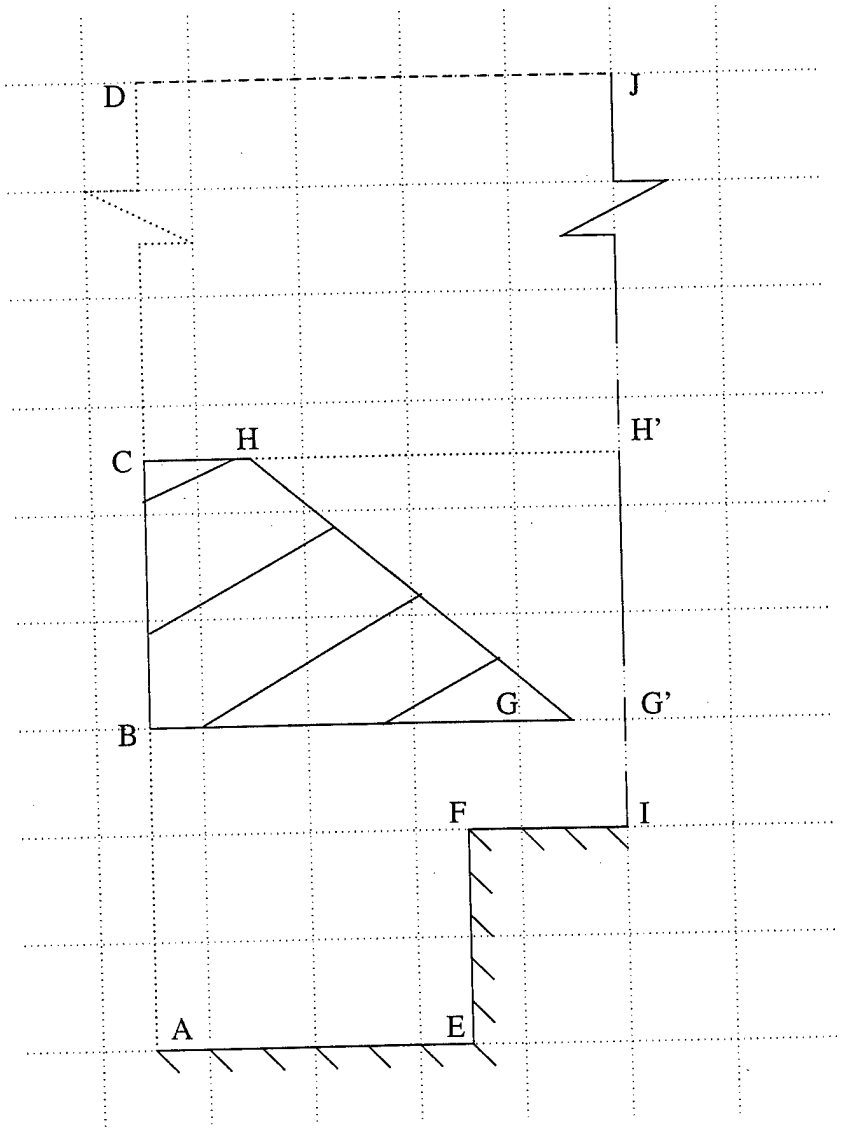
D
J
H
H'
C
G
G'
B
F
I
A
E

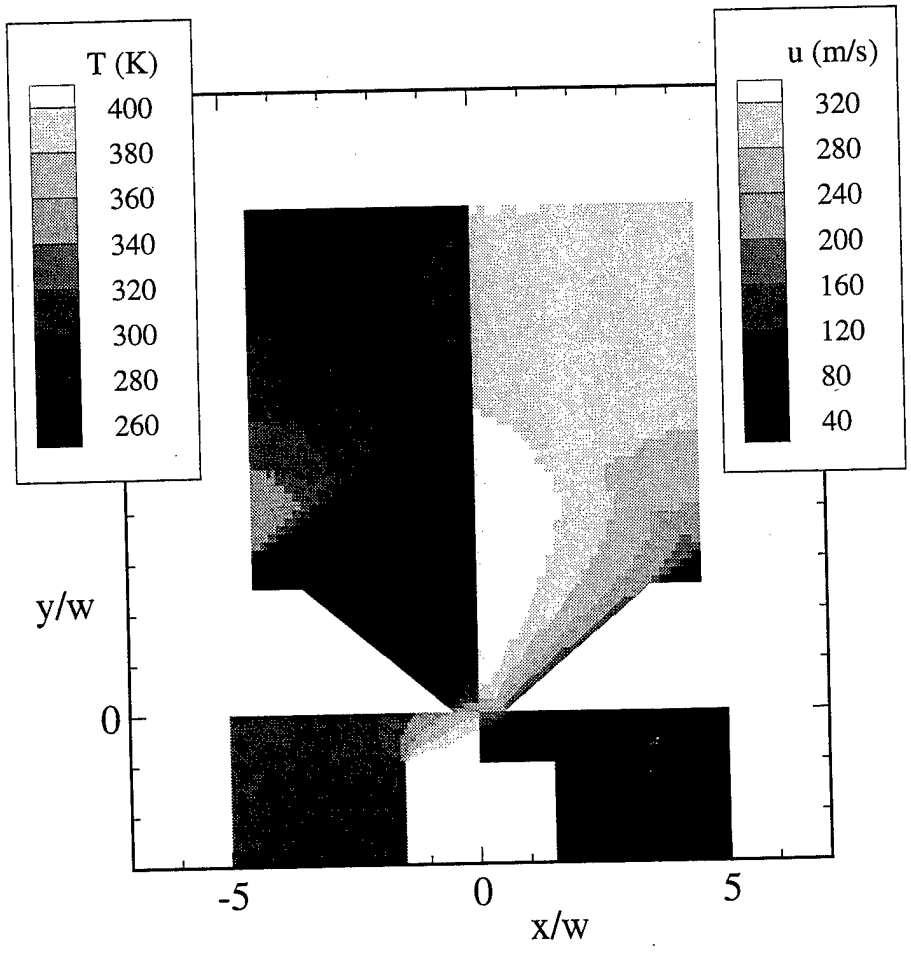
T (K)
400
380
360
340
320
300
280
260
u (m/s)
320
280
240
200
160
120
80
40
y/w
0
-5
0
5
x/w

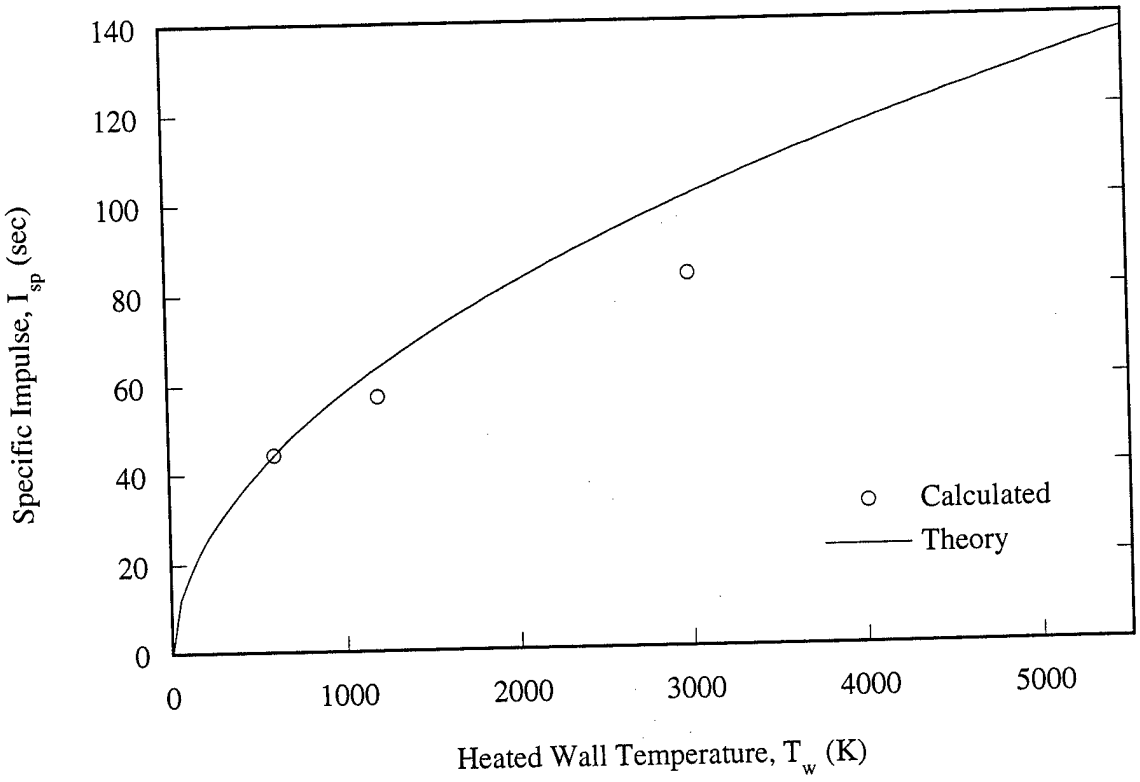
140
120
100
80
60
40
20
0
Specific Impulse, I_{sp} (sec)
0
1000
2000
3000
4000
5000
Heated Wall Temperature, T_w (K)
Calculated
Theory

Figure 4

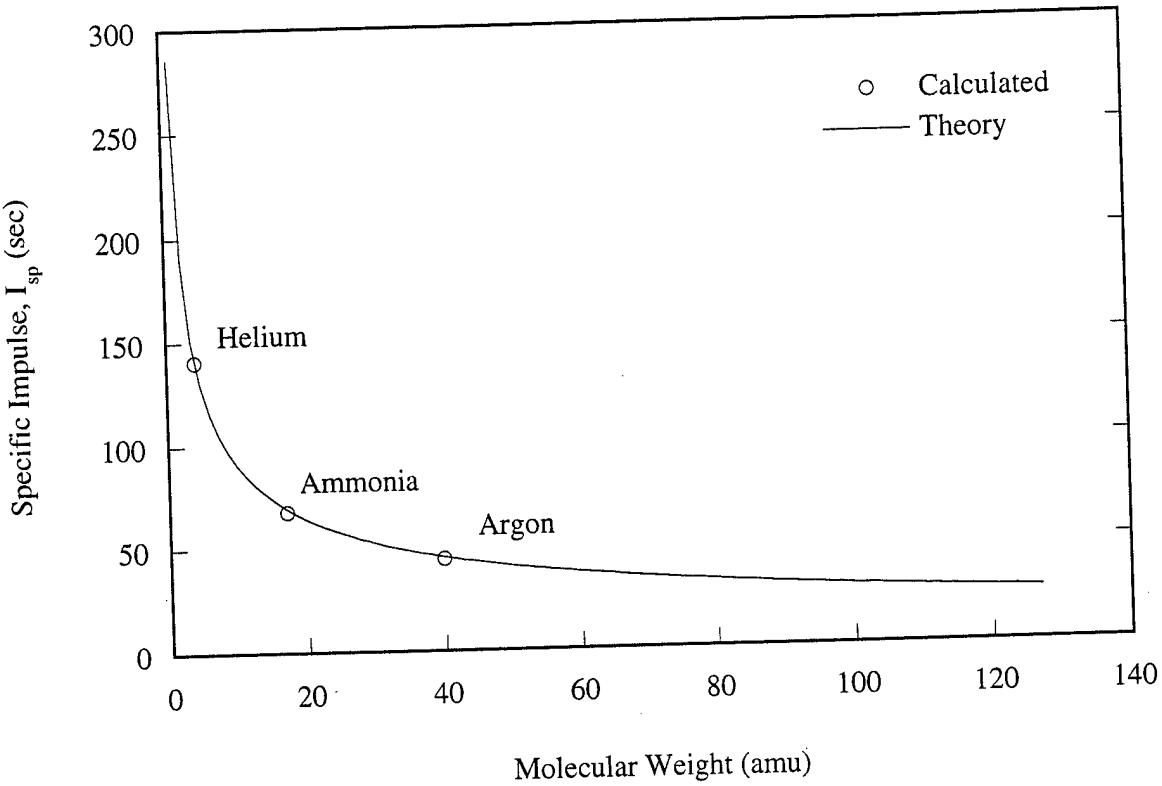
300
250
200
150
100
50
0
Specific Impulse, I_{sp} (sec)
0
20
40
60
80
100
120
140
Molecular Weight (amu)
Calculated
Theory
Helium
Ammonia
Argon

Figure 5

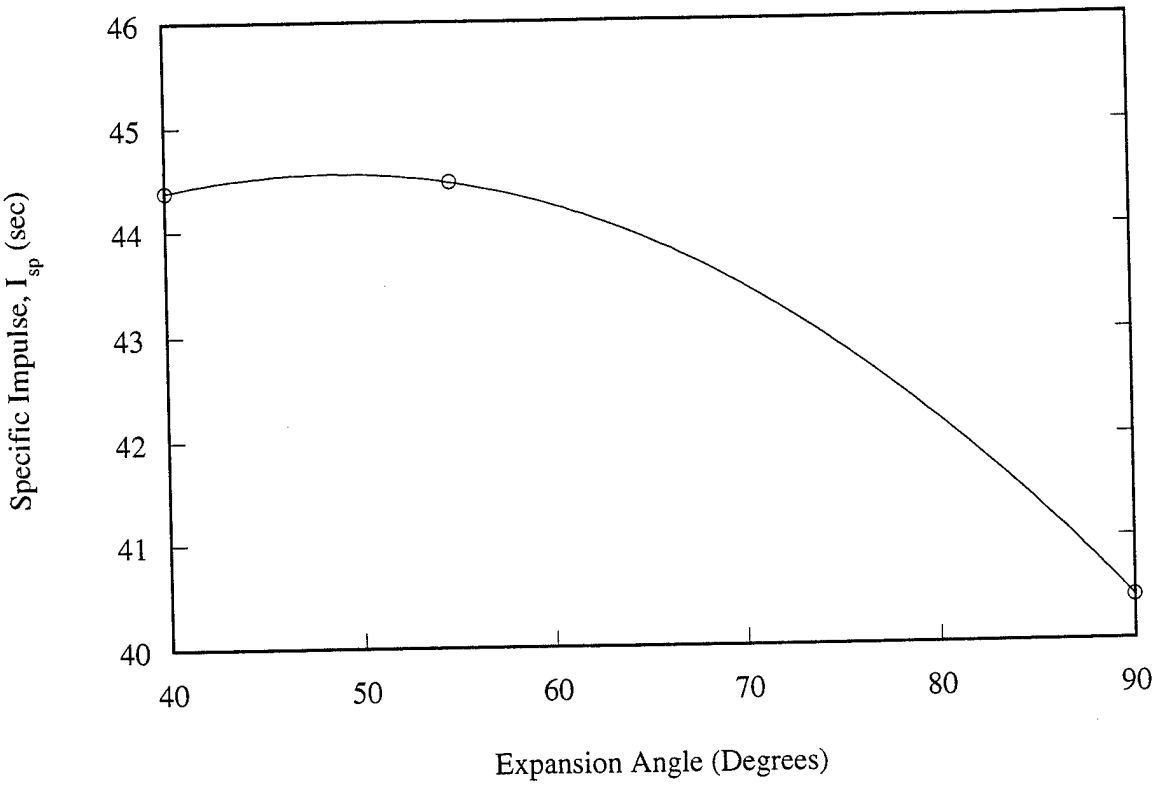
46
45
44
43
42
41
40
Specific Impulse, I_{sp} (sec)
40
50
60
70
80
90
Expansion Angle (Degrees)

Figure 6

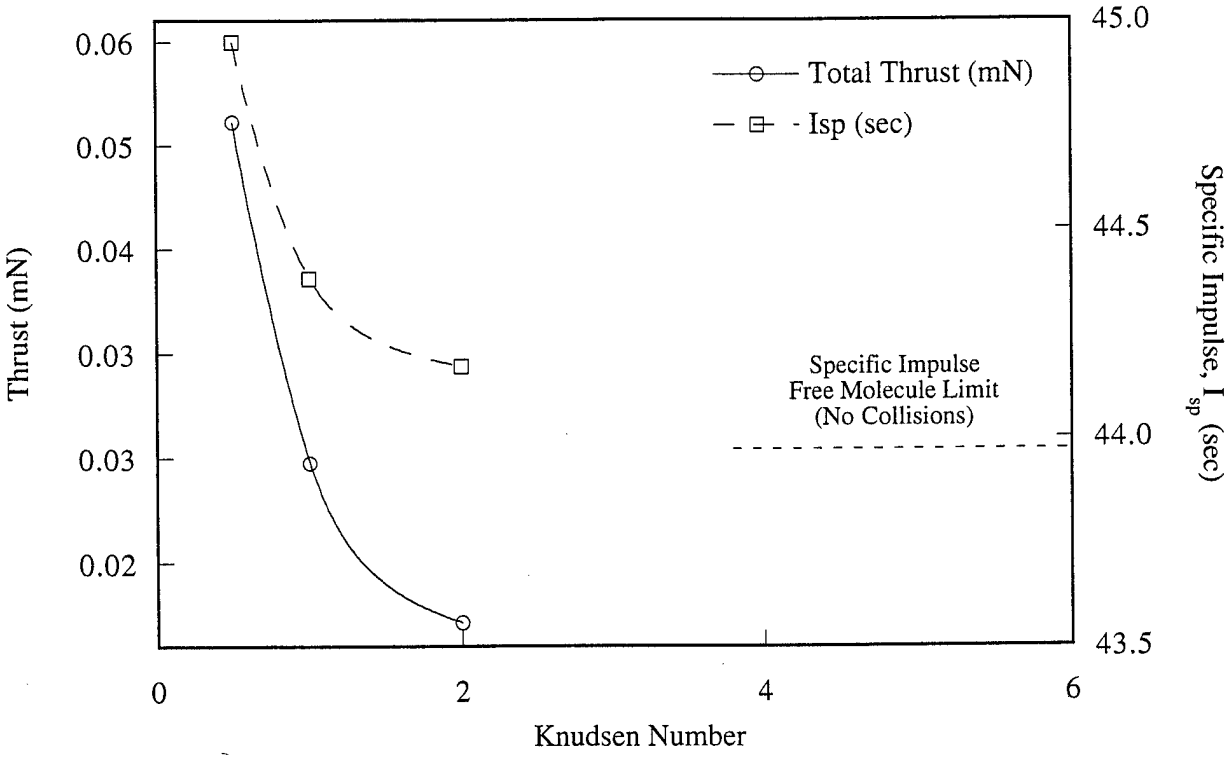
0.06
0.05
0.04
0.03
0.03
0.02
Thrust (mN)
45.0
44.5
44.0
43.5
Specific Impulse, I_{sp} (sec)
Total Thrust (mN)
Isp (sec)
Specific Impulse
Free Molecule Limit
(No Collisions)
0
2
4
6
Knudsen Number

Figure 7

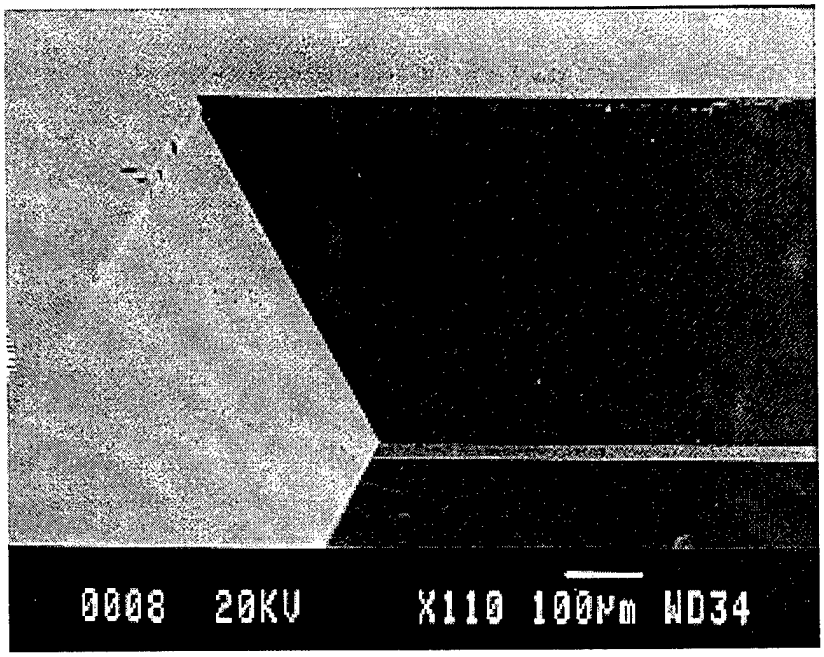

Figure 8

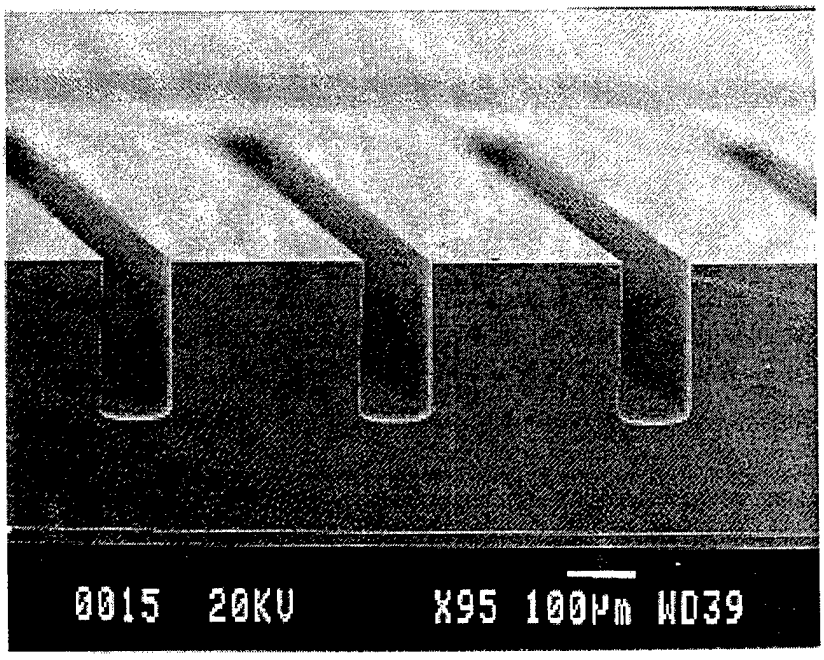

Figure 9